Aircraft anti-skid system modeling and simulation during landing runway path using Simcenter Amesim® and Bond Graphs for failure condition performance evaluation

Amorim J. P. F.[1], Fernandes A. B. F.[1], Trindade D. B.[1], Silva G. M.[1], Góes L. C. S.[1]

[1]*Dept. of Mechanical Engineering, Instituto Tecnológico de Aeronáutica*
50 Praça Marechal Eduardo Gomes, 12228-900, SP, Brazil
joaojpfa@ita.br, alessandra@ita.br, danieldbt@ita.br, gabrielmenezes@ita.br, lcsgoes@gmail.com

Abstract. Anti-skid is an electro-hydraulic control, applied in a brake system, that works to prevent aircraft wheels to lock and slip, mainly with runways under wet or icy conditions. Velocity sensors at the wheels measure its braking rates. If the speed decreases too rapidly, this could indicate wheel lock-up. In these situations, anti-skid control acts to relieve pressure at the brakes, so the wheels could be unlocked to prevent slipping.

A business aircraft was selected as a case study, in which the main landing gear system consists of 4 wheels (2 on each side). Brakes are operated by a hydraulic system, which is composed of two segregated hydraulic pressure sources, actuating on the internal and external wheels, respectively. This configuration prevents inadvertent yaw movements in the case of failure in one of the hydraulic sources.

The goal of the present work is to model an anti-skid system using bond graph methods and making subsequent computational modeling in Simcenter Amesim®. The model takes into account several effects such as the contact between tires and runaway; the contact between braking discs; braking disc thermal inertia; hydraulic actuator dynamics; hydraulic servo-valve dynamics and electric system PID control.

Keywords: aircraft, brake-system, anti-skid, system modeling, Amesim

1 Introduction

The anti-skid system compares the aircraft speed with the rotation speed of each wheel. If the speed of any wheel is too slow for the aircraft's speed, the brake is released so that the wheel speed increases and prevents the wheel from locking and slipping.

This system is automatic and activated immediately after the initial wheel spin on landing up to a limited minimum design speed. Another important feature is that such system removes the possibility of reverse skidding caused by locked wheels for different types of runway and weather conditions, thus enabling the runway length for landing not be so large.

An important factor for the anti-skid system is the slip (λ) which can be defined as the difference between the aircraft speed and the wheel speed, and it is calculated by eq. (1), where V_a is the aircraft velocity, ω represents the angular speed of the wheel and R is the radius of the wheel.

$$\lambda = \frac{Va - \omega R}{Va} \tag{1}$$

The control logic acts to maintain the slip level at a value where the system is stable and the friction coefficient is maximum. A good initial estimate might be to consider a reference value of 0.2. The friction coefficient curves used in our model are similar the ones found in Kiametis-Filho [1]. Each curve represents a runaway condition, being dependent on slip. These curves can be estimated by experiments or determined by equations which can be found in Kiametis-Filho [1] and are function of friction coefficient (μ), slip (λ) and constants that vary with runway condition.

When it comes to Amesim modeling, it is necessary to know some aircraft and braking system characteristics. Aircraft weight, wing area, lift and drag coefficients during landing phases, air density, touchdown speed, and lift

force reduced by the spoilers area are some of the main aircraft aspects. The main braking system attributes are the radius of the wheel, wheel moment of inertia, and the number of stators and rotors. The data used in this paper can be found in Kiametis-Filho [1] and then the anti-skid can be modeled.

This work is divided as follows: section 2 presents the modeling of the system under study using the Amesim software. Based on this, section 3 displays the results of this modeling for different track conditions. Section 4 uses Bond Graph modeling to represent the system and section 5 brings the conclusions of the study.

2 Amesim Model

The aircraft in question has two hydraulic systems for redundancy, with hydraulic system 1 feeding the inner wheels and hydraulic system 2 feeding the outer wheels of the main landing gear. The system is divided into two separate subgroups: one that represents the wheels and braking system, and another that represents the plane's mass. It is worth noting that the wheel subgroup is repeated four times to correspond to the number of wheels on the main landing gear. Each of these subgroups will be discussed further below.

The modeling of the brake system is shown in Fig. 4 and was based on the example described in LMS-AMESIM [2], which represents a hydraulic braking system for an aircraft in Rejected Take-Off condition, taking thermal effects into account. Additional models can also be found on the literature, like Maia-Neto and Góes [3]. Adaptations were made to consider both the aircraft's landing condition and the use of more than one brake system, one for each wheel. Another modification made was the addition of a proportional controller, which activates the servo valve based on the error signal between the system slip and the set point after one second of waiting, corresponding to the pilot's reaction time.

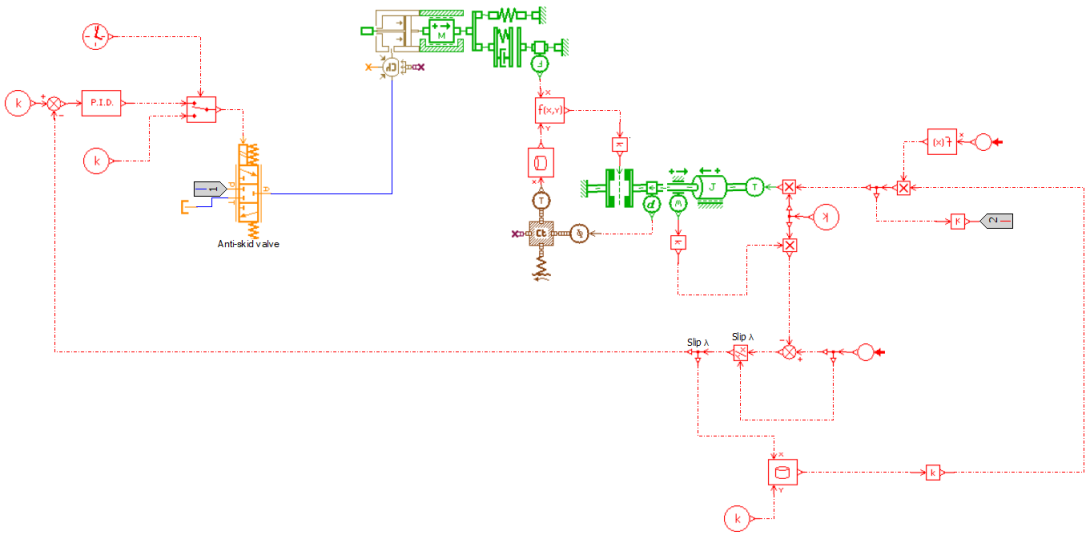

Figure 1. Modeling of the braking system

Different pressures are delivered to the actuator, which is represented by a piston, a mass, a return spring, and the brake contact surfaces, as shown in Fig. 2. The servo valve feeds a 3000-psi (2.07×10^7 Pa) pressure source to the actuator piston chamber to generate a positive left-to-right displacement for a positive control signal. For a negative control signal, the servo valve connects the actuator chamber to the return, decreasing the pressure in it, causing a right-to-left movement, pushed by the piston return spring.

As a result, the sign of the force applied to the contact surfaces is fed into a function that determines the effective contact force. This function also takes into account the temperature of the contact surfaces, which is caused by heat flux traveling through a thermal capacitance and is generated by energy dissipation on the surfaces. Then, the effective contact force is multiplied by a gain that represents the number of rotor-stator contact surfaces and then it is converted into a torque, which is linked to a rotational inertia that represents the wheel's mass.

In addition to the torque generated by the brake, the inertia of the wheel receives an opposite torque generated by the plane's movement. This torque is equal to the usual friction force multiplied by the radius of the wheel.

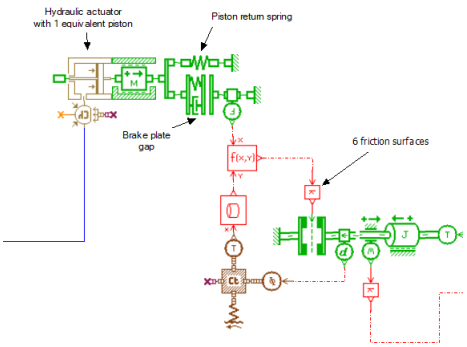

Figure 2. Details of modular representation for disc thermal effect and rotational disc dynamics

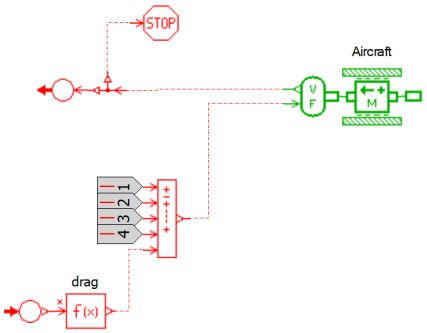

Figure 3. Plane's Modeling

The friction coefficient was multiplied by the normal force suffered to calculate the normal friction force. The coefficient of friction uses the formula represented in eq. (2) and is a function of the slip and the condition of the track, as mentioned above. The slip calculation is also fed back to the proportional control. Finally, the normal force used is described in eq. (3):

$$\mu(\lambda) = c_1(1 - e^{-c_2\lambda}) - c_3\lambda \qquad (2)$$

$$F_N = \frac{9.81 \cdot (0.85 \cdot M) - 0.5 \cdot \rho \cdot (0.2 \cdot C_L) \cdot S_{wing} \cdot V^2}{4} \qquad (3)$$

The 85% factor refers to the weight applied to the main landing gear, while the 20% factor comes from the lift generated by the wings, whereas spoilers reduce the total lift by 80%. The division by 4 takes place as it was considered that the force is divided equally between all the wheels of the main landing gear.

The aircraft modeling is represented in Fig 3. The mass was determined with the assumption that it receives friction force from the four wheels of the main landing gear plus the drag force, which is defined by eq. (4). In addition, a friction force in the mass was also configured, described by eq. (5):

$$D = 0.5 \cdot \rho \cdot C_D \cdot S_{wing} \cdot V^2 \qquad (4)$$

$$F_F = 0.1 \cdot 0.15 \cdot M \cdot 9.81 \qquad (5)$$

Finally, the mass sends its speed to each wheel. A simulation stop condition has also been added for when the airplane speed reaches 15 km/h, corresponding to a value 50% lower than the taxi speed recommended in Jordan et al. [4]. This modeling is also found in SUN et al. [5] and SHANG et al. [6].

3 Amesim Simulation

To analyze the system behaviour, five landing scenarios are simulated and described on the following sections. The simulation starts at the moment that the aircraft touches the runway. The proportional controller starts acting after 1 second of simulation.

3.1 Regular operation on a dry runway

The first simulation executed was aircraft landing during regular operation and on a dry runway. This was considered the standard scenario and it was used to better understand the expected results and system behavior. The results presented on Kiametis-Filho [1] were used as validation to the ones achieved. The parameters used were dry condition for the runway, 0.14 for slip setpoint, 2.07×10^7 Pa for line pressure and 61.7 m/s as initial velocity

The first aspect analyzed was the braking time and distance. The result achieved was 7.6 seconds and 287 meters, in comparison to 7.6 seconds and 279 meters, on the paper used as reference. Even with some differences between the simulation on Kiametis-Filho [1], the result for the standard landing condition differ very little.

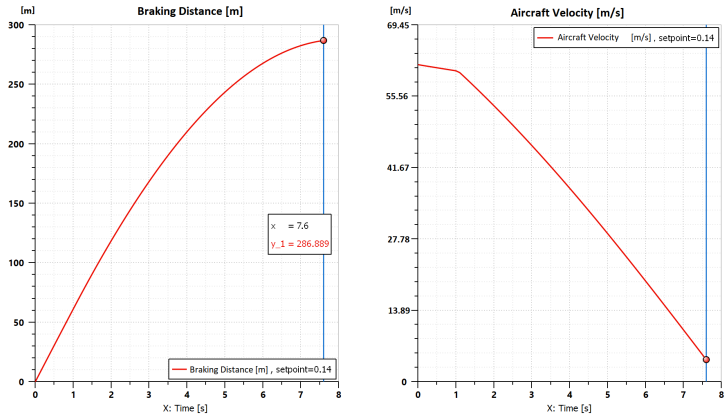

Figure 4. Dry condition aircraft kinematics results

There was a 2.9% difference in braking distance, and almost no difference on braking time. Thus, the model was considered satisfactory and representative. Also, the proportional controller was able to maintain the slip at the setpoint after approximately 0.5 s with a small overshoot. The pressure on the hydraulic systems lines reached approximately 1800 psi (1.24×10^7 Pa), staying under the 3000 psi limit. At last, the temperature on the discs was around 334 K.

3.2 Regular operation changing slip setpoint

This second round of simulations repeated the scenarios on section 3.1, but changing the slip setpoint. An optimal slip value will lead to better system performance. Values less than optimal will keep the system stable, but with degraded performance, while values higher than optimal tend to make the system more unstable. To observe this behavior, we evaluated five different slip values, being 0.08, 0.10, 0.12, 0.14 and 0.15. The results shown on table 1 describe the simulation time necessary to achieve the stop condition and the distance traveled. It is possible to conclude that the closest value to the optimal is slip is 0.14, presenting the smaller braking distance and simulation time. Also, at 0.15 setpoint, the controller was not able to stabilise the slip value through most of the simulation, just controlling it after 6 seconds.

Table 1. Regular operation changing slip setpoint

Slip setpoint	0.08	0.1	0.12	0.14	0.15
Braking Distance [m]	305.9	295.8	289.9	286.9	289.6
Braking time [s]	8.3	7.9	7.7	7.6	7.6

3.3 Regular operation on different runway conditions

The third simulation compares the plane's braking performance for different types of runway. The tracks analyzed were dry, wet and snowy tracks. with a different friction coefficient curve for each condition. The slip setpoint was also adjusted closest to its optimal values, being 0.14 to the dry condition, 0.08 to the wet condition and 0.03 to the snowy condition. As expected for the snowy runway, which has the lowest friction coefficient, it was the case where the aircraft took the longest time to stop. The system was able to brake the aircraft under dry and wet conditions, but under snowy condition, it was only able to bring it under 12.5 m/s after 30 s.

Table 2. Regular operation on different runway conditions

Runway condition	Dry	Wet	Snowy
Braking time [s]	7.6	10.7	30
Final velocity [m/s]	4.28	4.31	12.50

3.4 Regular operation with different aircraft landing weight

The fourth simulation consists of analyzing the difference in braking performance for different weights. The original landing weight of 13,500 kg, MTOW of 17400 kg and a hypothetical value of 30,000 kg, which is used only for comparison purposes since the aircraft is not capable of reaching this weight. The slip setpoint was fixed at 0.14 for all cases. Even with a weight more than twice larger, the system is capable of braking the aircraft to a velocity under 4.17 m/s with a slight change in time. However, it interesting to notice that for the first two conditions, the hydraulic systems pressures stayed under the 3000 psi, but for the 30,000 kg scenario reach the limit. Due this limitation, the controller was not able to reach the 0.14 slip setpoint, stabilizing on a 0.07 slip.

Table 3. Regular operation with different aircraft landing weight

Aircraft Weight [kg]	13,500	17,400	30,000
Braking time [s]	7.6	7.4	8.3
Max. Line press [Pa]	1.26×10^7	$1,59 \times 10^7$	2.07×10^7
Slip	0.14	0.14	0.07

3.5 One of the hydraulic systems failed on dry runway

The last simulation consists of analyzing the failure of one of the hydraulic systems under a standard dry runway condition. It was noticed that, compared to normal operation, the failure of one of the hydraulic systems leads to an increase of 200 meters and 6 seconds for braking. However, the controller was capable to keep the slip at 0.14 and did not reach the 3000 psi limit. Another aspect to be notice is the brake system temperature, that was a raise from 343 K, under regular operation to 383 K, due to the longer time it takes to brake the plane and the overload on one of the brake systems.

4 Bond Graph Model

As presented in section 2, an Amesim simulation was developed to model the aircraft behavior. To further investigate the energy domains implicated in this system, a Bond Graph model was created using 20sim software, and is presented in Figure 5. This model includes the following physics:

1. **Mechanical domain:**
   - 3-way servo-valve spool linear second order dynamics
   - Linear actuator dynamics
   - Discs and tire rotational dynamics
   - Simplified aircraft dynamics
2. **Hydraulic domain:** 3-way servo-valve hydraulic lines dynamics
3. **Thermal domain:** temperature dependant disc-clamp friction coefficient
4. **Electrical domain:** PID controller for servo-valve spool actuation

The PID is used for modulating an electric motor (GY) responsible for transducing electric current into force, acting on the servo-valve spool positioning. The spool dynamic considers spool mass inertia (inductance *I1*), damping (resistance *R1*) and return spring (conductance *C1*). Spool speed (Junction 1) signal is integrated, resulting in the spool positioning over time.

This positioning is then used as modulating signal for the servo-valve pressure drop. This way, through the spool positioning, it is possible to control hydraulic flow rate within the valve. The hydraulic piping are composed by three parts: supply, return and actuator lines. All of those are modeled considering line pressure losses (*R2*, *R3* and *R8*) and compressibility effects (*C*, *C6* and *C7*). For positive spool positioning, supply and actuator lines are connected, as the hydraulic supply pressure (represented by effort source *Se - supply*) is imposed on the actuator. When spool positioning is negative, actuator line is connected to return line, and pressure is released from actuator to return line (represented by effort source *Se - return*).

Hydraulic pressure is transformed in brake force by an area coefficient, which acts in the actuator linear second order dynamics. Inertia (*I2*), Damping (*R4*) and spring (*C1*) effects are modeled. Actuator is modeled by two points: the hydraulic line interface and the friction contact with the disc. Between these two points, the model also takes into account stiffness along actuator body, represented by resistance *R5* and capacitance *C5*. A 1 mm

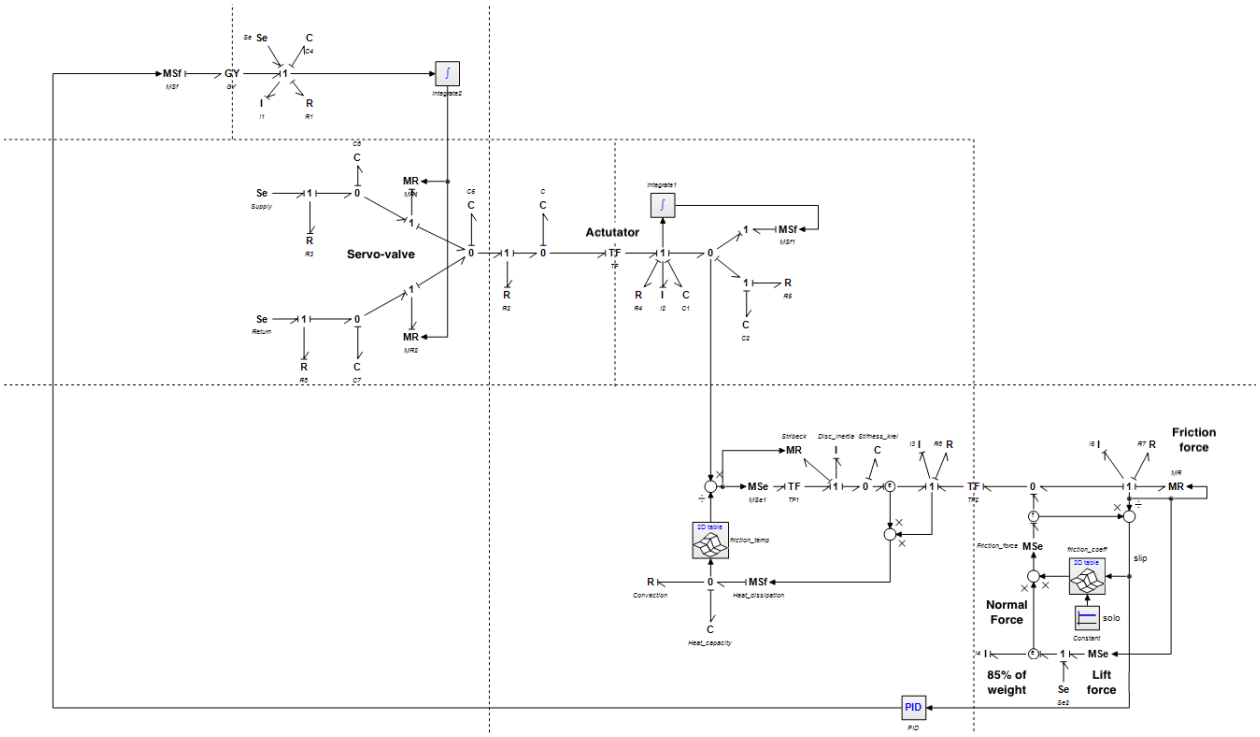

Figure 5. Bond Graph model developed with 20sim software

gap between actuator contact path and discs is also modeled, representing the fact that the discs are not always in contact with the actuator. As the actuator contact patch moves towards the disc, this gap is closed, and contact is established. This behavior is represented by modulated flux source *MSf1*. When the distance between contact patch and disc is bellow 1 mm, actuator and contact patch move with the same speed. When contact is established, the actuator contact patch speed becomes zero, indicating that the contact point is not allowed to move any further. The details of BG representation are shown in Figure 6.

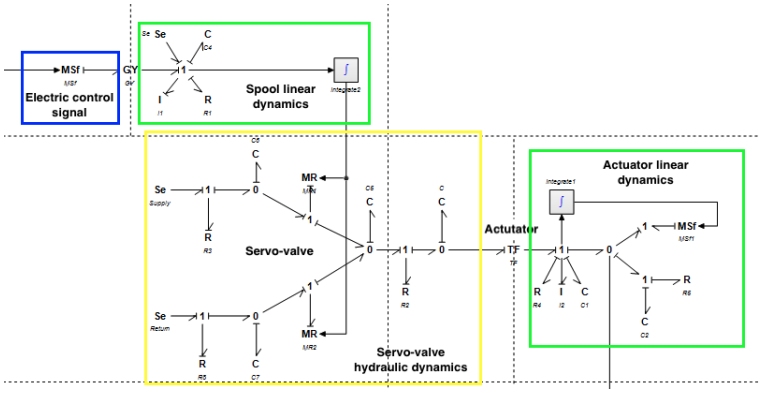

Figure 6. Details of BG representation for hydraulic line and actuator

The contact force is than transformed in torque by a medium arm and friction coefficients. The friction coefficient is a function of disc temperature. This thermal domain effect also takes into account disc body heat capacity (capacitance C), convection with air (resistance R) and heat dissipated from braking. Torque is applied on disc, influencing its rotational dynamics, which also considers disc inertia (inductance *I*) and Stribeck effect (resistance *MR*). The linkage between disc and tire considers stiffness (capacitance *C k_rel*). Tire dynamics is also modeled with inertia (inductance *I3*) and dissipation effects (resistance *R5*). The details of BG representation are shown in Figure 7.

Tires receive the effect of both braking forces and reaction forces from the aircraft dynamics. As a result,

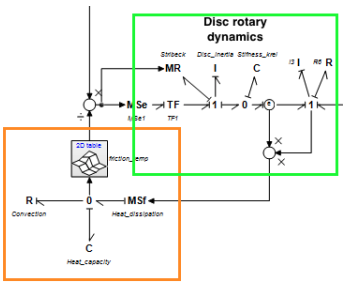

Figure 7. Details of BG representation for disc thermal effect and rotational disc dynamics

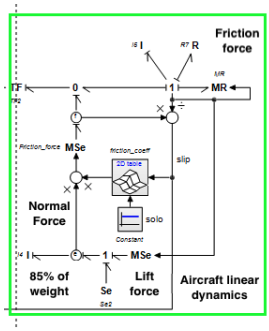

Figure 8. Details of BG representation for aircraft linear dynamics and slip calculation

the aircraft is simply modeled by a single mass point, considering inertia (inductance *I5*) and dissipation effects (resistance *R7*). As shown in Figure 8, slip is computed from aircraft and tire velocities. Friction force derives from friction coefficient and normal force on ground. According to Kiametis-Filho [1], normal force is considered as 85% of aircraft weight. The tire-ground friction coefficient is a function of tire slip (represented by *friction_coeff* 2D table), and the PID controller uses slip signal for slip regulation though the modulation of braking force, preventing wheel blockage. The details of BG representation are shown in Figure 8.

BG modeling provides a systematic method for multi-domain characterization, allowing a better understanding of all phenomena involved in the system.

5 Conclusion

The first step in achieving the goal of this work was to understand the behavior of the anti-skid system, as well as to analyze the variables and physical phenomena present in the system. The system was represented using Amesim software, and this model can be considered representative since it was validated through comparisons with both the Amesim demo model and data from the literature. The modeling described here took into account various runway conditions by utilizing equations that connect the friction coefficient with the slip coefficient. It is vital to note that an experimental curve of these two parameters is conceivable. Another significant condition exposed during this study was the system's behavior in the event of a hydraulic system failure. Finally, a Bond Graph model was proposed to represent the characteristics of the model used in the Amesim software. Future studies will involve simulating Bond Graph model and comparing it to Amesim results, as well as studying more failure conditions, such as hydraulic leakage failures, profiting from the possibilities of BG modeling.

Authorship statement. The authors hereby confirm that they are the sole liable persons responsible for the authorship of this work, and that all material that has been herein included as part of the present paper is either the property (and authorship) of the authors, or has the permission of the owners to be included here.

References

[1] D. Kiametis-Filho. Development of an anti-skid controller based on wheel sleep. Master's thesis, Institute Tecnológico de Aeronáutica, Praça Marechal Eduardo Gomes, São José dos Campos - SP, Brazil, 12228-900, 2017.

[2] LMS-AMESIM. Braking system: Rejected take off step 2: Thermal effect, 2016.

[3] M. Maia-Neto and L. C. S. Góes. Use of lms amesim model and a bond graph support to predict behavior impacts of typical failures in an aircraft hydraulic brake system. *Journal of the Brazilian Society of Mechanical Sciences and Engineering*, vol. 40, n. 414, 2018.

[4] R. Jordan, M. A. Ishutkina, and T. G. Reynolds. A statistical learning approach to the modeling of aircraft taxi time. In *29th Digital Avionics Systems Conference*, pp. 1.B.1–1–1.B.1–10, 2010.

[5] D. SUN, Z. JIAO, Y. SHANG, S. WU, and X. LIU. High-efficiency aircraft antiskid brake control algorithm via runway condition identification based on an on-off valve array. *Chinese Journal of Aeronautics*, vol. 32, n. 11, pp. 2538–2556, 2019.

[6] Y. SHANG, X. LIU, Z. JIAO, and S. WU. A novel integrated self-powered brake system for more electric aircraft. *Chinese Journal of Aeronautics*, vol. 31, n. 5, pp. 976–989, 2018.